

Study of Cationic *N*-Isopropylacrylamide–Styrene Copolymer Latex Particles Using Fluorescent Probes

E. M. S. Castanheira,^{†,‡} J. M. G. Martinho,^{*,†} D. Duracher,[§] M. T. Charreyre,[§] A. Elaïssari,[§] and C. Pichot^{*,§}

Centro de Química-Física Molecular, Complexo I, Instituto Superior Técnico, Av. Rovisco Pais, 1049-001 Lisboa, Portugal, and Unité Mixte CNRS-bioMérieux, ENS de Lyon, 46 Allée d'Italie, 69364 Lyon Cedex 07, France

Received February 9, 1999. In Final Form: May 24, 1999

Monodisperse cationically charged core–shell poly[styrene/*N*-isopropylacrylamide] latexes, differing in their shell structure, were studied at temperatures around the lower critical solution temperature (LCST) of poly[*N*-isopropylacrylamide]. Near the LCST, a transition on the latex dimensions was observed by quasi-elastic light scattering measurements. The same transition could also be detected using the intensity ratio of the pyrene fluorescence vibronic bands, I_1/I_3 , and the excimer to monomer fluorescence intensity ratio of 1,10-bis(1-pyrenyl)decane. The fluorescence spectra and decay curve measurements of 1,10-bis(1-pyrenyl)decane provided a better understanding of both the hydrophilic–hydrophobic variation and the conformational changes occurring in the poly[*N*-isopropylacrylamide] shell of the latex particles upon temperature variation.

Introduction

Among polymeric microspheres offering suitable properties as carriers for biologically active macromolecules, poly[*N*-isopropylacrylamide (NIPAM)] microgels were found to exhibit outstanding capabilities, especially due to their thermal sensitivity. In the last years, these latexes have attracted much attention, motivated by the dramatic change of their colloidal properties (particle size, electrophoretic mobility, colloidal stability, etc.) upon temperature variation.^{1–4} These changes take place around the lower critical solution temperature (LCST), near 32 °C for pure poly[NIPAM], which corresponds to the coil–globule transition of poly[NIPAM] chains, induced by the dehydration of amide moieties. However, in the case of microgel particles containing numerous entangled polymer chains, the transition is not as sharp as that for free polymer in solution, due to their colloidal nature: presence of ionic interfacial charges, confined environment of macromolecules, cross-linking, etc. This has motivated several studies to characterize the interfacial hydrogel layer.^{5,6}

At CNRS-bioMérieux laboratory we have recently explored the properties of reactive core–shell latex particles, where the hydrophobic core of polystyrene (PS) is covered by a poly[NIPAM] shell. The systematic work already done has the objective of characterizing these thermosensitive particles for use as supports for diagnostics. In a first paper,⁷ the preparation of monodisperse cationic amino-containing poly[S/NIPAM] core–shell par-

ticles was thoroughly investigated and it was evidenced that the polymerization process (batch versus shot-growth) dictates the particle size and morphology. By combination of transmission, scanning, and atomic force microscopy techniques, it was shown that these hydrophilic particles could sometimes exhibit odd-shaped structures depending on the process performed and composition of the latex recipe.

In subsequent papers,^{8,9} it was found that pH, temperature, and ionic strength strongly modify the colloidal behavior of such cationic core–shell particles, especially the electrokinetic properties and the colloidal stability. Nevertheless, the understanding of the phenomenon is incomplete due to the structural complexity of the poly[NIPAM]-rich shell of these particles. In addition, a better knowledge of the hydrophilic–lipophilic balance (HLB) of the shell, particularly upon changing temperature, is crucial when considering the interactions of these thermosensitive latexes with biomolecules.

The influence of temperature on the properties of poly[NIPAM] hydrogels has been studied by contact angle measurements and fluorescence techniques. Contact angle measurements reflect the HLB variation around the LCST and were made by Fujimoto et al.¹⁰ and by Zhang et al.¹¹ on macrogels. On the other hand, fluorescence measurements of probes incorporated in these materials give relevant information of the local medium surrounding the probe. Pyrene-labeled poly[NIPAM] chains were systematically studied by Winnik et al. around the LCST in water.^{12,13} Fujimoto et al.¹⁰ pioneered the investigation of poly[NIPAM] microspheres in comparison with linear poly[NIPAM] chains in solution. They studied, using 8-aminonaphthalene-1-sulfonic acid (ANS), the influence of salt

* To whom correspondence should be addressed.

[†] Centro de Química-Física Molecular, Complexo I, Instituto Superior Técnico.

[‡] Present address: Departamento de Física, Universidade do Minho, Campus de Gualtar, 4700-320 Braga, Portugal.

[§] Unité Mixte CNRS-bioMérieux, ENS de Lyon.

(1) Pelton, R. H.; Pelton, H. M.; Morphis, A.; Rowell, R. L. *Langmuir* **1989**, *5*, 816.

(2) Kawaguchi, H.; Fujimoto, K.; Mizuhara, Y. *Colloid Polym. Sci.* **1992**, *270*, 53.

(3) McPhee, W.; Tam, K. C.; Pelton, R. *J. Colloid Interface Sci.* **1993**, *156*, 24.

(4) Makino, K.; Yamamoto, S.; Fujimoto, K.; Kawaguchi, H.; Ohshima, H. *J. Colloid Interface Sci.* **1994**, *166*, 251.

(5) Zhu, P. W.; Napper, D. H. *J. Colloid Interface Sci.* **1994**, *168*, 380.

(6) Zhu, P. W.; Napper, D. H. *J. Colloid Interface Sci.* **1996**, *177*, 343.

(7) Duracher, D.; Sauzedde, F.; Elaïssari, A.; Perrin, A.; Pichot, C. *Colloid Polym. Sci.* **1998**, *276*, 219.

(8) Duracher, D.; Sauzedde, F.; Elaïssari, A.; Pichot, C.; Nabzar, L. *Colloid Polym. Sci.* **1998**, *276*, 920.

(9) Nabzar, L.; Duracher, D.; Elaïssari, A.; Chauveteaux, G.; Pichot, C. *Langmuir* **1998**, *14*, 5062.

(10) Fujimoto, K.; Nakajima, Y.; Kashiwabara, M.; Kawaguchi, H. *Polym. Int.* **1993**, *30*, 237.

(11) Zhang, J.; Pelton, R.; Deng, Y. *Langmuir* **1995**, *11*, 2301.

(12) (a) Winnik, F. M. *Macromolecules* **1990**, *23*, 233. (b) Winnik, F. M. *Macromolecules* **1990**, *23*, 1647.

(13) Barros, T. C.; Adronov, A.; Winnik, F. M.; Bohne, C. *Langmuir* **1997**, *13*, 6089.

concentration in the LCST of hydrogel microspheres and showed that above the LCST the medium is more hydrophobic. Fluorescence quenching by nitromethane allowed them to prove that poly[NIPAM] microgels protect more the probe than free polymer chains in solution. This indicates that the probe can penetrate into the cross-linked hydrogel, reflecting its fluorescence the inner environment of the hydrogel. Recently, Pankansen et al.¹⁴ used the sensitivity to the microenvironment of pyrene fluorescence spectrum vibronic bands to follow the hydrophobicity of poly[NIPAM] colloidal microgels with temperature around the LCST. In addition, fluorescence quenching of both pyrene and tris(bipyridine)ruthenium was used to show that the probe stays in an aqueous environment below the LCST, while above the LCST is distributed between the aqueous phase and the more hydrophobic poly[NIPAM] gel.

This paper aims to report fluorescence studies for monodisperse cationically charged core-shell poly[S/NIPAM] latexes differing in their shell structure, with the purpose of characterizing the hydrogel shell. Two latexes, one with a cross-linked shell (DD4) and other without cross-links (DD1), were studied. Initially, the variation of the latexes diameter with temperature was obtained by quasi-elastic light scattering (QELS). Afterward, steady-state and time-resolved fluorescence experiments were performed at several temperatures around the LCST of poly[NIPAM], using both pyrene and 1,10-bis(1-pyrenyl)decane probes.

2. Experimental Section

2.1. Materials. 1,10-Bis(1-pyrenyl)decane from Molecular Probes was used as received. Pyrene (Kock-Light, 99% pure) was zone refined (100 steps). The probes were solubilized in ethanol (Merck Uvasol) to obtain 10^{-5} M stock solutions. The incorporation of the probes in water was achieved by solvent evaporation of the stock solutions, prior to the addition of the latexes.

A batch emulsifier-free emulsion polymerization process was used to prepare the DD1 latex. Boiled and deoxygenated water (200 mL) was introduced into a 250 mL round-bottomed four-necked reactor equipped with a glass anchor-shaped stirrer, condenser, and nitrogen inlet, under a constant stream of nitrogen. Styrene (18 g) and *N*-isopropylacrylamide (2 g) were then added. After temperature equilibrium at 70 °C, the solution was stirred for 30 min before introducing the initiator, 2,2'-azobis(amidinopropane) dihydrochloride (V50) (0.2 g). The reaction was carried out for 24 h.

The DD4 latex was prepared by a shot-growth polymerization process. At the beginning, the polymerization was carried out as for DD1. After 89% of conversion, boiled and deoxygenated water (25 g), *N*-isopropylacrylamide (5.07 g), *N,N*-methylenebisacrylamide (MBA, cross-linker) (0.069 g), aminoethyl methacrylate hydrochloride (AEM, cationic amino containing monomer) (0.147 g), and the initiator 2,2'-azobis(amidinopropane) dihydrochloride (0.122 g) were added. The detailed procedure, recipe, and kinetic study of the polymerization of these systems were reported recently.^{7,8}

The cationic polystyrene latex^{8,15} was synthesized under the same batch emulsifier-free conditions. Boiled and deoxygenated water (200 mL) was introduced into the reactor with distilled styrene (18 g). The initiator 2,2'-azobis(amidinopropane) dihydrochloride (0.2 g) was then added, and the reaction proceeds for 24 h.

Following a similar procedure, the cross-linked poly[NIPAM] microgel¹⁶ was synthesized by introducing in the reactor 200 mL of boiled and deoxygenated water, 4 g of *N*-isopropylacrylamide, and 0.32 g of MBA. The initiator (V50, 0.04 g) was added to start the polymerization, which was carried out during 6 h.

All latexes were cleaned by repetitive centrifugation and redispersion using deionized Milli-Q grade water, before any characterization study, to remove free electrolytes and water-soluble polymers.

Diluted dispersions of latex particles ($C \sim 5 \times 10^{-6}$ g/mL) in Milli-Q grade water were prepared for QELS and fluorescence measurements. The ionic strength was kept at 10^{-3} M NaCl, to reduce the electrostatic repulsions between the ionic groups randomly distributed along the polyelectrolyte chains.

The fluorescent probes, 1,10-bis(1-pyrenyl)decane and pyrene, were introduced at very low concentration (10^{-7} M) in aqueous dispersions of these latexes.

2.2. Methods. Quasi-elastic light scattering (QELS) measurements were made in a standard multiangle laser light scattering equipment from Brookhaven Instruments, Inc. The light source was a 35 mW He-Ne laser, which produces vertical polarized light at $\lambda = 632.8$ nm (Spectra-Physics, model 127). The scattering cells (10 cm³ cylindrical ampules) were immersed in a Decalin bath, with temperature control (accuracy better than 0.5 °C) by water circulation (Neslab, model RTE-110). The signal analyzer consists of a 128 channel autocorrelator (Brookhaven, model 2030AT), where the last six channels are used for baseline calculations.

The intensity autocorrelation function $G^{(2)}(\tau)$ has the form¹⁷

$$G^{(2)}(\tau) = A[1 + B|g^{(1)}(\tau)|^2] \quad (1)$$

where A is the baseline, B a spatial coherence factor, τ the delay time, and $g^{(1)}(\tau)$ the first-order normalized electric field time correlation function.

For a polydisperse system, $g^{(1)}(\tau)$ consists of a sum of single exponentials

$$g^{(1)}(\tau) = \int_0^\infty G(\Gamma) \exp(-\Gamma\tau) d\Gamma \quad (2)$$

where $G(\Gamma)$ is the normalized distribution function of decay rates, Γ . The z -average translational diffusion coefficient, D_z , can be obtained from $\Gamma = D_z q^2$, knowing the magnitude of the scattering vector, $q = (4\pi n/\lambda) \sin(\theta/2)$. The intensity autocorrelation plots of diluted latex solutions of refractive index, n , were obtained at a scattering angle of $\theta = 90^\circ$. The autocorrelation traces were analyzed with the regularized non-negatively constrained least-squares method (CONTIN) to obtain the size distribution based on the hydrodynamic diameter of the latexes. The mean hydrodynamic diameters at temperature T were calculated from the translational diffusion coefficients at infinite dilution using the Stokes-Einstein equation, $d = k_B T / (3\pi\eta D_z)$, knowing the Boltzmann constant, k_B , and the viscosity, η , of the medium. For each sample, at least five autocorrelation traces were measured at each temperature, being the deviation of the hydrodynamic radius always lower than 7%.

Fluorescence spectra were recorded at several temperatures with a Spex Fluorolog F112A spectrofluorometer, equipped with a double emission monochromator and a home-built thermostating unit. The temperature of the cuvette (1 cm \times 1 cm) was controlled with an accuracy better than 0.2 °C. The samples were maintained at least 30 min at each temperature (after temperature stabilization), before the measurements. The bandwidths for both excitation and emission were 1.8 nm.

Time-resolved picosecond fluorescence decays were recorded by the single-photon timing technique with laser excitation at 330 nm. The apparatus consists of a mode-locked Coherent Innova 400-10 argon-ion laser that synchronously pumped a cavity dumped Coherent 701-2 DCM dye laser, delivering 5–6 ps pulses (with ≈ 40 nJ/pulse) at a repetition rate of 460 kHz.

The monomer ($\lambda_{em} = 377$ nm) and excimer ($\lambda_{em} = 520$ nm) fluorescence were selected by a Jobin-Yvon HR320 monochromator with a grating of 100 lines/mm. The detector used was a Hamamatsu 2809U-01 microchannel plate photomultiplier. The instrument response function had an effective full width at half maximum of 35 ps.

(16) Meunier, F.; Elaïssari, A.; Pichot, C. *Polym. Adv. Technol.* **1995**, *6*, 489.

(17) (a) Chu, B. *Laser Light Scattering, Basic Principles and Practice*, 2nd ed.; Academic Press Inc.: New York, 1991. (b) Johnson, C. S., Jr.; Gabriel, D. A. *Laser Light Scattering*; Dover: New York, 1994.

(14) Pankansen, S.; Thomas, J. K.; Snowden, M. J.; Vincent, B. *Langmuir* **1994**, *10*, 3023.

(15) Ganachaud, F.; Sauzedde, F.; Elaïssari, A.; Pichot, C. *J. Appl. Polym. Sci.* **1997**, *65*, 2315.

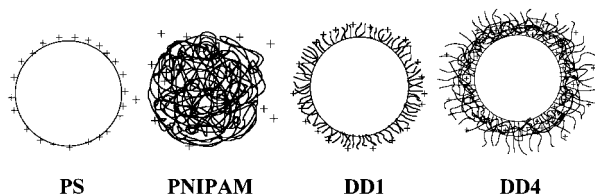


Figure 1. Schematic illustration of prepared latex particles: PS, polystyrene; PNIPAM, cross-linked poly(NIPAM); DD1, core-shell poly(S/NIPAM), with a thin shell; DD4, core-shell poly(S/NIPAM), with cross-linked thicker shell.

Table 1. Characteristics of Latex Particles

sample	cationic groups	diameter, d_h (nm)		δ^a (nm)
		at 20 °C	at 50 °C	
PS	amidine	300	300	0
PNIPAM	amidine	560	300	130
DD1	amidine	362	322	20
DD4	amidine and amine	552	360	96

$$^a \delta(\text{nm}) = (d_{h,20^\circ\text{C}} - d_{h,50^\circ\text{C}})/2.$$

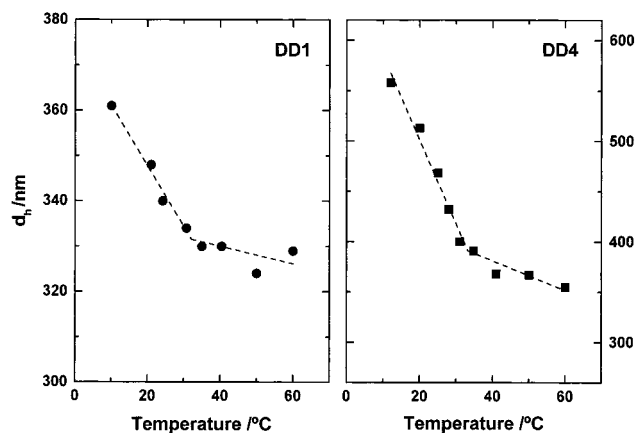


Figure 2. Hydrodynamic diameter of core-shell poly(S/NIPAM) latex particles DD1 (●) and DD4 (■), between 10 and 60 °C.

Decay curves were analyzed using an iterative reconvolution method based on the algorithm of Marquardt.¹⁸

3. Results and Discussion

3.1. Characteristics of the Latex Particles. The DD1 and DD4 latexes are core-shell latex particles with a polystyrene core (PS) and a poly[NIPAM] shell. The structure of these particles is schematically presented in Figure 1. The DD4 latex bears a thick cross-linked shell, while DD1 has a smaller non-cross-linked poly[NIPAM] shell. All the particles exhibit a positive surface charge.

The distribution of diameters obtained by QELS is unimodal and very narrow for both latexes, with polydispersities of 1.007 (DD1) and 1.011 (DD4). Table 1 shows the diameters of a PS particle, a poly[NIPAM] cross-linked microgel, and DD1 and DD4 latexes, at 20 and 50 °C, obtained by QELS. The particles containing poly[NIPAM] shrink upon temperature increase, but not the PS particle. Therefore, the thermal sensitivity of DD1 and DD4 is due to the poly[NIPAM] shell.

3.2. Quasi-Elastic Light Scattering (QELS). Figure 2 shows the variation with temperature of the hydrodynamic diameter of DD1 and DD4 core-shell latex particles, measured by QELS between 10 and 60 °C. The particle size decreases rapidly until ≈ 32 °C and then very slowly for higher temperatures. The change in size is due to the

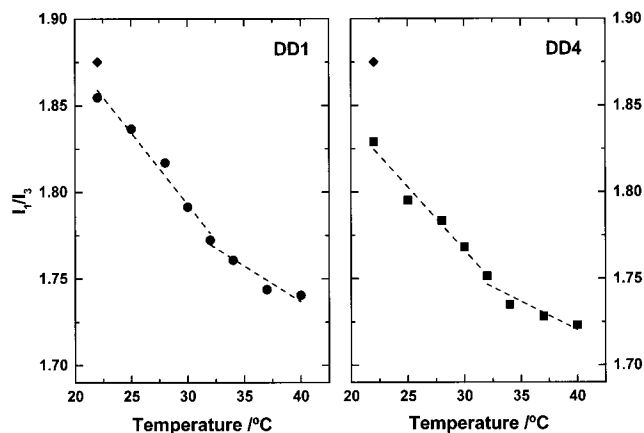


Figure 3. Fluorescence intensity ratio of pyrene vibronic bands, I_1/I_3 ($\lambda_{\text{exc}} = 334$ nm), as a function of temperature, in aqueous dispersions of DD1 (●) and DD4 (■) latexes. (◆) I_1/I_3 for pyrene in water at 22 °C.

shrinkage of the poly[NIPAM] shell, induced by dehydration of isopropylamide moieties in the hydrogel. The transition temperatures of 32.1 °C for DD1 and 33.1 °C for DD4 were calculated from the intercept of the two straight lines in Figure 2. These values are close to the LCST of poly[NIPAM] in water (~ 32 °C).^{4,12,19,20}

However, the latex transition is expected to be broad,¹⁻⁴ compared to the very sharp coil-globule transition of poly[NIPAM] single chain in water.¹⁹ This difference was attributed to the presence of positive charges that should modify the transition of the interfacial chains.^{5,6} Moreover, for DD4 the conformational changes should also be influenced by the heterogeneous cross-linking of poly[NIPAM] chains within the shell layer.

The slightly higher transition temperature of DD4 (systematically found) compares well with the transition temperature for the cross-linked poly[NIPAM] hydrogel (33.5 °C). This fact indicates that cross-links influence the conformational changes induced by temperature variation.

3.3. Steady-State Fluorescence Measurements.

Fluorescence spectra of 1,10-bis(1-pyrenyl)decane and pyrene introduced in latex dispersions at very low concentration (10^{-7} M) were obtained at several temperatures. The ratio of the fluorescence intensity of the vibronic bands, $I_1(0 \rightarrow 0)$ and $I_3(2 \rightarrow 0)$, of pyrene reflects the polarity of the local medium, increasing with polarity.²¹

Figure 3 shows the variation of this ratio (I_1/I_3) with temperature for DD1 and DD4 latex dispersions prepared at 22 °C. The ratio decreases with temperature, the variation being steeper until 32 °C. This clearly shows that pyrene is in a more hydrophobic medium at higher than at lower temperatures. The I_1/I_3 ratio is always lower than the value reported for pyrene in water, $I_1/I_3 = 1.87$,²¹ showing that in both latex dispersions the medium is less hydrophilic than water. At low temperatures, the I_1/I_3 ratio for DD1 is higher than that for DD4, but at 40 °C a similar value was obtained for both latexes (1.72 for DD4 and 1.74 for DD1). This shows that at low temperatures the DD4 shell is more hydrophobic than the DD1 shell, while at temperatures higher than 40 °C the hydrophobicity of both latexes is similar.

The transition temperatures can be obtained from the intercept of two straight lines (Figure 3). The values calculated for DD1 (33.5 °C) and DD4 (33.3 °C) are close

(19) Wu, C.; Zhou, S. *Macromolecules* **1995**, *28*, 8381.

(20) Fujishige, S.; Kubota, K.; Ando, I. *J. Phys. Chem.* **1989**, *93*, 3311.

(21) Dong, D. C.; Winnik, M. A. *Can J. Chem.* **1984**, *62*, 2560.

(18) Marquardt, D. W. *J. Soc. Ind. Appl. Math.* **1963**, *11*, 431.

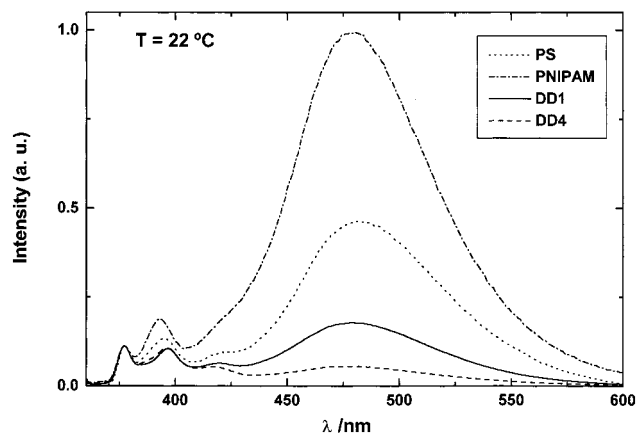


Figure 4. Fluorescence spectra of 1,10-bis(1-pyrenyl)decane ($\lambda_{\text{exc}} = 346$ nm) at 22 °C in dispersions of cationic PS (···), cross-linked PNIPAM (---), DD1 (—), and DD4 (— · —). The spectra were normalized at 377 nm.

to those obtained by QELS. The differences can be explained by the large uncertainty on these values due to the small variation of I_1/I_3 in this temperature range.

The intramolecular excimer formation process of 1,10-bis(1-pyrenyl)decane should also give information on the hydrophilic/hydrophobic character of the core-shell latex particles. Indeed, in a hydrophilic medium is expected a higher excimer to monomer fluorescence intensity ratio, I_E/I_M , owing to the tendency of the pyrenes linked by the methylene chain to be in proximity or even to form dimers.²² Nevertheless, a lower value of the I_E/I_M ratio can also reflect the lower mobility of the probe chain ends imposed by the structure of the medium.

The steady-state fluorescence spectra of 1,10-bis(1-pyrenyl)decane in several polymer colloid dispersions at room temperature are displayed in Figure 4. The large excimer to monomer fluorescence intensity ratio observed for the poly[NIPAM] hydrogel dispersion suggests that the probe is in contact with water. The lower value obtained for the polystyrene dispersion indicates that the probe is adsorbed onto the PS surface, indicating a more hydrophobic environment. The even lower excimer intensity observed in core-shell latex particles is a good indication that the probe is located near the polystyrene core coated by the poly[NIPAM] chains.

It should be noted that a stationary fluorescence spectrum is obtained only after several hours for polystyrene and poly[NIPAM] hydrogel particles, while for the core-shell latexes the corresponding time is inferior to 30 min. Until the stationary state is attained, the monomer and excimer emission intensities vary in time, this being particularly visible for the excimer. In water, a stationary fluorescence spectrum was not reached even after 1 day, and several bands could be observed in the excimer emission region, showing the presence of excited dimers and excimers with different configurations. These results demonstrate that our high hydrophobic probe is essentially incorporated in the latex spheres.

Figure 5 shows the fluorescence spectra of 1,10-bis(1-pyrenyl)decane in the DD1 dispersion at several temperatures. The probe was introduced in the latex dispersion at 22 °C, being afterward heated until 40 °C. The decrease with temperature of the excimer to monomer fluorescence intensity ratio reflects a more hydrophobic probe environment at higher temperatures, resulting from the shrinkage of poly[NIPAM] hairs with a dehydration

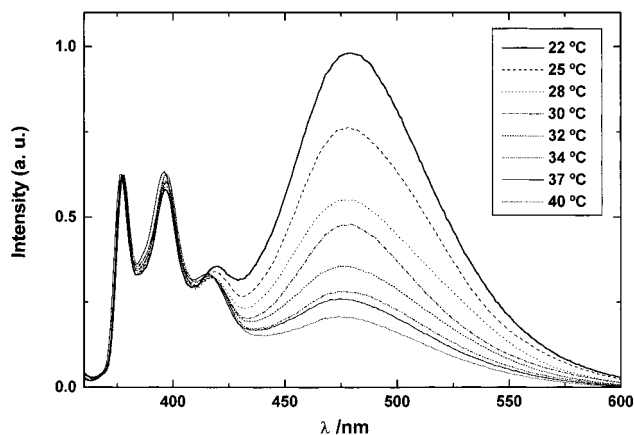


Figure 5. Fluorescence spectra of 1,10-bis(1-pyrenyl)decane ($\lambda_{\text{exc}} = 346$ nm) in a dispersion of core-shell latex DD1, at several temperatures. The spectra were normalized at 377 nm.

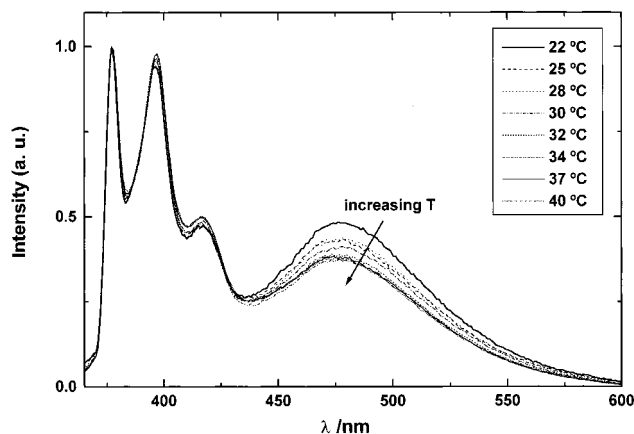


Figure 6. Fluorescence spectra of 1,10-bis(1-pyrenyl)decane ($\lambda_{\text{exc}} = 346$ nm) in a dispersion of core-shell latex DD4, at several temperatures. The spectra were normalized at 377 nm.

of the poly[NIPAM] chains. However, a small contribution for this decrease should come from the diminution of the pyrene-labeled chain ends diffusion.

For dispersions of the DD4 latex, a similar trend was observed for the fluorescence spectra (Figure 6), upon increasing temperature. Nevertheless, a much smaller variation with temperature of the excimer to monomer fluorescence intensity ratio was observed. This reflects the difference in shell structure between the latexes, the larger cross-linked shell of DD4 appearing more hydrophobic than the non-cross-linked shell of DD1.

The variation of the I_E/I_M ratio with temperature, presented in Figure 7, allows the determination of transition temperatures of 32.1 °C for DD1 and 33.3 °C for DD4, in very good agreement with the values obtained from QELS measurements. The similarity of transition temperatures obtained with and without the probe (by fluorescence and QELS, respectively) shows that the probe does not disturb the poly[NIPAM] chain shrinkage and collapse.

The values of I_E/I_M in DD1 and DD4 dispersions are practically equal at 40 °C, suggesting that the probe is in a similar environment in both cases, which corresponds to a condensed hydrophobic collapsed structure of the poly[NIPAM] chains.

To predict how pyrene dimers influence the results, the excitation spectra of the probe were recorded at 377 nm (monomer emission) and 480 nm (excimer emission). Figure 8 shows that the spectrum recorded at 377 nm is blue-shifted by about 2 nm for the DD1 dispersion and 1

(22) Ilharco, L. M.; Martins, C. I.; Fedorov, A.; Martinho, J. M. G. *Chem. Phys. Lett.* **1997**, *277*, 51.

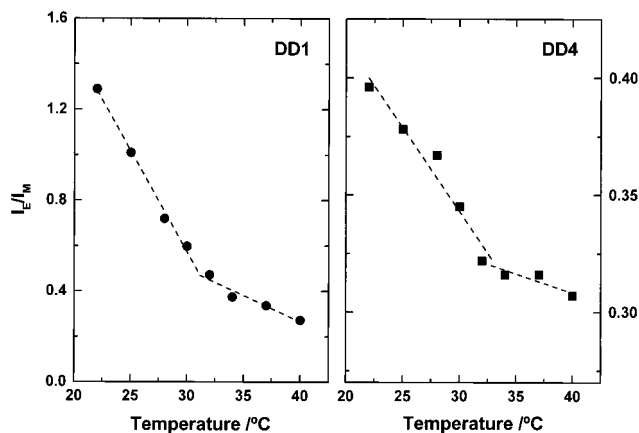


Figure 7. Ratio of excimer (500 nm) to monomer (377 nm) fluorescence intensities, I_E/I_M , of 1,10-bis(1-pyrenyl)decane ($\lambda_{exc} = 346$ nm) as a function of temperature, in aqueous dispersions of DD1 (●) and DD4 (■) latexes.

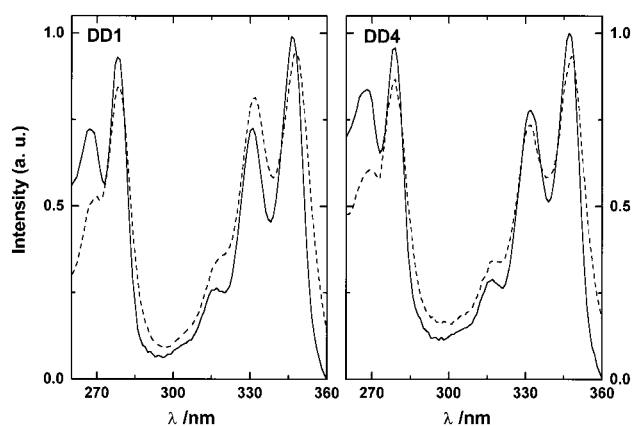


Figure 8. Excitation spectra of 1,10-bis(1-pyrenyl)decane in DD1 and DD4 dispersions at 25 °C: (—) $\lambda_{em} = 377$ nm, (---) $\lambda_{em} = 480$ nm.

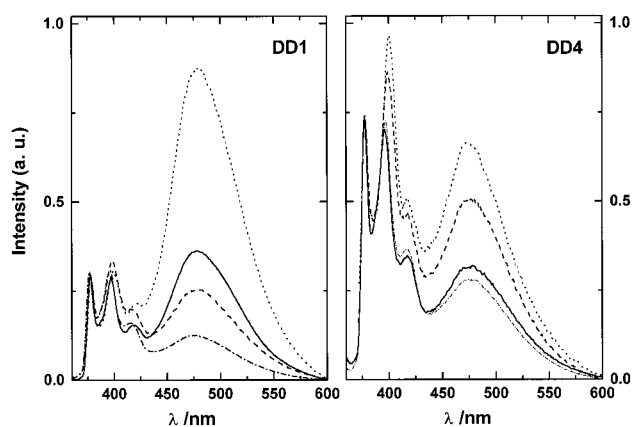


Figure 9. Normalized fluorescence spectra of 1,10-bis(1-pyrenyl)decane in DD1 and DD4 dispersions, at $\lambda_{exc} = 346$ nm and $\lambda_{exc} = 355$ nm, before (25 °C) and after (37 °C) the transition: 25 °C (—) $\lambda_{exc} = 346$ nm, (···) $\lambda_{exc} = 355$ nm; 37 °C (---) $\lambda_{exc} = 346$ nm, (-·-·) $\lambda_{exc} = 355$ nm.

nm for DD4. This indicates that the emission at 480 nm comes not only from dynamic excimers formed by a diffusive process of the methylene chain ends but also from excited pyrene dimers.²²

The same conclusion can be extracted from the fluorescence spectra at $\lambda_{exc} = 355$ nm presented in Figure 9. The shape of the spectrum in the monomer emission region shows the emission of excited preassociated pyrene dimers, which absorb a larger fraction of the excitation light at

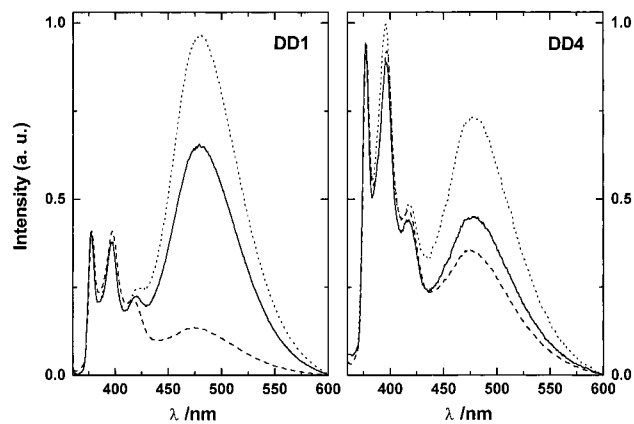


Figure 10. Normalized fluorescence spectra of 1,10-bis(1-pyrenyl)decane in DD1 and DD4 dispersions ($\lambda_{exc} = 346$ nm): probe added at 22 °C (before transition), 22 °C (—) and 40 °C (---); probe added at 40 °C (after transition), 40 °C (···).

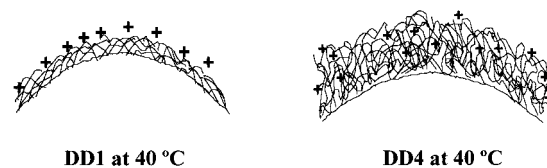


Figure 11. Schematic illustration of the structure of DD1 and DD4 shell at 40 °C.

355 nm but not at 346 nm. Indeed, the pyrene dimer to monomer relative absorption is higher at $\lambda_{exc} = 355$ nm, since the pyrene $S_1 \leftarrow S_0$ transition in the long wavelength region is symmetry forbidden, with a very low molar absorption coefficient. The Raman scattering of water, which should appear at 404 nm by excitation at 355 nm, is too small to justify the rise in emission intensity around 400 nm. The emission from preassociated pyrene dimers ($\lambda_{exc} = 355$ nm) is more visible in DD4 than in DD1. This is attributed to a faster conversion of the excited dimers to excimers in DD1 and reflects the cross-linked structure of the DD4 shell, which restricts the mobility of the probe.

At 37 °C, the I_E/I_M ratio remains higher by excitation at 355 nm than by excitation at 346 nm, confirming the presence of pyrene ground-state dimers even at this temperature. Nevertheless, a similar I_E/I_M ratio (around 0.65) was observed for both latexes ($\lambda_{exc} = 355$ nm), suggesting a similar probe environment in both DD1 and DD4 latexes at this temperature.

To verify if poly[NIPAM] chains are completely collapsed at 40 °C, 1,10-bis(1-pyrenyl)decane was added to the latex dispersions, previously heated at 40 °C. Figure 10 shows the fluorescence spectra of the probe incorporated in both latex dispersions at 22 and at 40 °C. The spectra show that the probe is in a more hydrophilic medium when added to the dispersions at 40 °C than at 22 °C. Therefore, at 40 °C, the shrunken poly[NIPAM] hairs prevent the probe from penetrating deeply into the poly[NIPAM] shell.

Nevertheless, when the probe is incorporated at 40 °C, the I_E/I_M values for DD4 are much smaller than those for DD1. This suggests a noncompletely collapsed DD4 shell at 40 °C due to the cross-links and the presence of many charges along the poly[NIPAM] chains. The probes seem to be located in a more hydrophobic medium in DD4 than in DD1, showing that the probes penetrate inside the collapsed shell in DD4 but not in DD1, where they are more exposed to water. The drawing presented in Figure 11 is an attempt to show the expected collapsed shell structures of DD1 and DD4, in agreement with the observation derived from the fluorescence measurements.

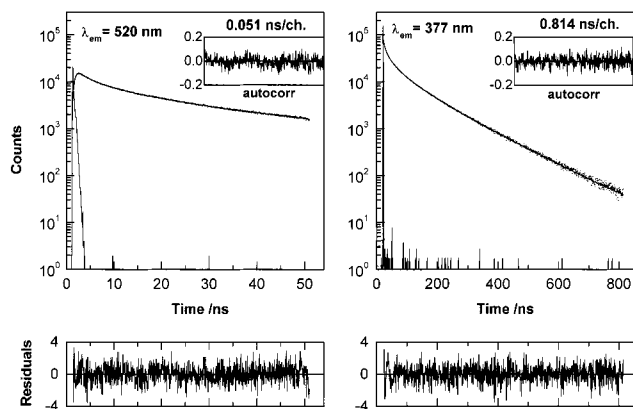


Figure 12. Fluorescence decay curves of excimer and monomer of 1,10-bis(1-pyrenyl)decane in a dispersion of DD1 at 22 °C, fitted with a sum of exponentials (a_i , pre-exponential factor; τ_i , lifetime). Excimer: $a_1 = -0.208$, $\tau_1 = 0.33$ ns; $a_2 = 0.144$, $\tau_2 = 2.9$ ns; $a_3 = 0.136$, $\tau_3 = 15.5$ ns; $a_4 = 0.053$, $\tau_4 = 62.1$ ns; $\chi^2 = 1.16$. Monomer: $a_1 = 0.430$, $\tau_1 = 0.33$ ns; $a_2 = 0.025$, $\tau_2 = 2.9$ ns; $a_3 = 0.019$, $\tau_3 = 14.7$ ns; $a_4 = 0.014$, $\tau_4 = 55.4$ ns; $a_5 = 0.009$, $\tau_5 = 133$ ns; $\chi^2 = 1.13$.

3.4. Fluorescence Decay Measurements. To complement the information from fluorescence spectra, decay curve measurements of 1,10-bis(1-pyrenyl)decane in both core-shell latex dispersions were performed, at the monomer (377 nm) and excimer (520 nm) emission wavelengths, below and above the transition temperature. The decays were recorded at time scales of 0.051 and 0.210 ns/channel for the excimer and 0.210 and 0.814 ns/channel for the monomer, using a multichannel analyzer operating with 1024 channels.

Figure 12 shows the excimer and monomer decays of 1,10-bis(1-pyrenyl)decane in DD1 latex dispersion at 22 °C. The excimer decay curve is very complex and can only be fitted as a sum of four exponentials. A very short rise time component (≈ 330 ps) is observed, resulting from the diffusion of pyrenes linked to the same methylene chain to form a dynamic excimer. The very small rise time indicates that the pyrene chain ends are very close. This is evidence that the medium is highly hydrophilic, forcing the approach of the pyrene chain ends. The three other components have lifetimes of 2.9, 15.5, and 62.1 ns.

The monomer decay has to be fitted as a sum of five exponentials. When the two short components of the excimer decay are fixed (0.33 and 2.9 ns), the recovered lifetimes are 14.7, 55.4, and 133 ns. The first two recovered lifetimes are close to those obtained from the excimer decay, showing multiequilibria between the species (monomer, excimer, and dimers). The longest component, absent in the excimer decay, is attributed to isolated monomers, which decay with an intrinsic lifetime of ≈ 130 ns (in the presence of oxygen).

For DD4 at 22 °C, the excimer and monomer decay curves are similar to those of DD1 at the same temperature. However, the rise time of the excimer decay is ≈ 380 ps, clearly higher than in DD1, indicating a decrease of the formation rate of dynamic excimers in DD4. Therefore, the average distance between the pyrene-labeled ends of the probe should be larger in DD4 (more hydrophobic medium than in DD1) and/or the DD4 cross-linked shell imposes more restrictions to the methylene chain ends mobility.

The decay curves of the probe in DD1 dispersion at 40 °C are reported in Figure 13. The rise time of the excimer decay (510 ps) increased by about 200 ps compared to the value at 22 °C, showing that the pyrene chain ends are further apart and/or the mobility of chain ends decreased

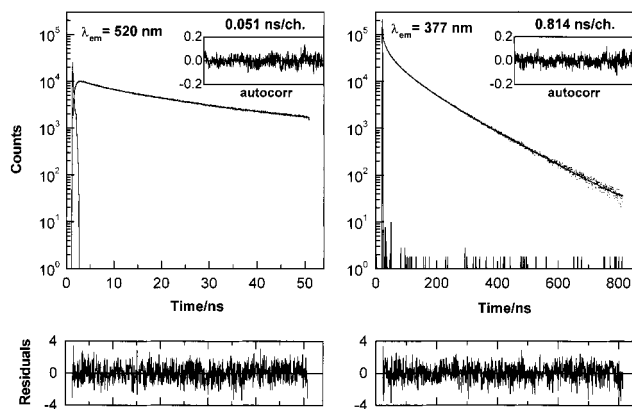


Figure 13. Fluorescence decay curves of excimer and monomer of 1,10-bis(1-pyrenyl)decane in a dispersion of DD1 at 40 °C, fitted with a sum of exponentials (a_i , pre-exponential factor; τ_i , lifetime). Excimer: $a_1 = -0.137$, $\tau_1 = 0.51$ ns; $a_2 = 0.029$, $\tau_2 = 3.7$ ns; $a_3 = 0.053$, $\tau_3 = 19.0$ ns; $a_4 = 0.025$, $\tau_4 = 54.3$ ns; $\chi^2 = 1.18$. Monomer: $a_1 = 0.186$, $\tau_1 = 0.51$ ns; $a_2 = 0.020$, $\tau_2 = 3.7$ ns; $a_3 = 0.017$, $\tau_3 = 16.3$ ns; $a_4 = 0.013$, $\tau_4 = 55.3$ ns; $a_5 = 0.008$, $\tau_5 = 125$ ns; $\chi^2 = 1.04$.

due to the collapse of the poly[NIPAM] chains. At 40 °C, the rise times are very similar for both DD1 (510 ps) and DD4 (530 ps) dispersions, which confirms the existence of a similar probe environment at this temperature, in accordance to the steady-state fluorescence measurements.

4. Conclusions

The hydrophilic/hydrophobic character and structure of the hairy shell of cationically charged core-shell poly[S/NIPAM] latexes were studied using pyrene and 1,10-bis(1-pyrenyl)decane as fluorescent probes. The I_1/I_3 fluorescence intensity ratio of pyrene was used to follow the hydrophobicity of the medium surrounding the probe. The 1,10-bis(1-pyrenyl)decane excimer to monomer fluorescence intensity ratio reflects both the hydrophobicity and the structure of the poly[NIPAM] shell.

The steady-state fluorescence data allow the calculation of transition temperatures, around 32 °C for DD1 (non-cross-linked shell) and 33 °C for DD4 (cross-linked shell). These values agree with those obtained by QELS. The transition temperature seems to increase with the cross-linking and the charge density of the shell, which impose different collapse modes to the poly[NIPAM] chains.

Fluorescence decay curve measurements of 1,10-bis(1-pyrenyl)decane introduced in DD1 and DD4 dispersions are complex, due to the multiequilibria between monomers, dimers, and excimer species. Nevertheless, the results confirm that, around the transition temperature, the shell structure changes due to the collapse of the poly[NIPAM] chains. The structure of the collapsed chains seems to be more compact for DD1 than for DD4, which was attributed to the cross-links and the higher charge density along the polymer chains of DD4.

The wettability of these particles is currently being evaluated by contact angle measurements. Both contact angle and fluorescence measurements may offer a better knowledge of the interface of these core-shell latexes with relevance for the adsorption-desorption processes of biomolecules onto their surface.

Acknowledgment. J. M. G. Martinho is grateful for the support of this work from FCT. E. M. S. Castanheira acknowledges FCT for a grant (PRAXIS XXI/BPD/9968/96).